

## Structure-function assessment of mannosylated poly(beta-amino esters) upon targeted antigen presenting cell gene delivery

Charles H. Jones, Mingfu Chen, Akhila Gollakota, Anitha Ravikrishnan, Guojian Zhang, Sharon Lin, Myles Tan, Chong Cheng, Haiqing Lin, and Blaine A. Pfeifer

*Biomacromolecules*, **Just Accepted Manuscript** • DOI: 10.1021/acs.biomac.5b00062 • Publication Date (Web): 07 Apr 2015

Downloaded from <http://pubs.acs.org> on April 11, 2015

### Just Accepted

“Just Accepted” manuscripts have been peer-reviewed and accepted for publication. They are posted online prior to technical editing, formatting for publication and author proofing. The American Chemical Society provides “Just Accepted” as a free service to the research community to expedite the dissemination of scientific material as soon as possible after acceptance. “Just Accepted” manuscripts appear in full in PDF format accompanied by an HTML abstract. “Just Accepted” manuscripts have been fully peer reviewed, but should not be considered the official version of record. They are accessible to all readers and citable by the Digital Object Identifier (DOI®). “Just Accepted” is an optional service offered to authors. Therefore, the “Just Accepted” Web site may not include all articles that will be published in the journal. After a manuscript is technically edited and formatted, it will be removed from the “Just Accepted” Web site and published as an ASAP article. Note that technical editing may introduce minor changes to the manuscript text and/or graphics which could affect content, and all legal disclaimers and ethical guidelines that apply to the journal pertain. ACS cannot be held responsible for errors or consequences arising from the use of information contained in these “Just Accepted” manuscripts.

1  
2  
3  
4  
5  
6  
7  
8  
9  
10  
11  
12  
13  
14  
15  
16  
17  
18  
19  
20  
21  
22  
23  
24  
25  
26  
27  
28  
29  
30  
31  
32  
33  
34  
35  
36  
37  
38  
39  
40  
41  
42  
43  
44  
45  
46  
47  
48  
49  
50  
51  
52  
53  
54  
55  
56  
57  
58  
59  
60

# Structure-function assessment of mannosylated poly(beta-amino esters) upon targeted antigen presenting cell gene delivery

*Charles H. Jones<sup>‡</sup>, Mingfu Chen<sup>‡</sup>, Akhila Gollakota, Anitha Ravikrishnan, Guojian Zhang, Sharon Lin, Myles Tan, Chong Cheng, Haiqing Lin, Blaine A. Pfeifer\**

Department of Chemical and Biological Engineering, University at Buffalo, The State University of New York, Buffalo, New York, USA

Keywords: Gene therapy, nonviral vector, cationic polymers, antigen presenting cells, poly(beta-amino esters)

1  
2  
3 ABSTRACT  
4  
5  
6

7 Antigen presenting cell (APC) gene delivery is a promising avenue for modulating  
8 immunological outcomes towards a desired state. Recently, our group developed a delivery  
9 methodology to elicit targeted and elevated levels of APC-mediated gene delivery. During these  
10 initial studies, we observed APC-specific structure-function relationships with the vectors used  
11 during gene delivery that differ from current non-APC cell lines, thus emphasizing a need to re-  
12 evaluate vector-associated parameters in the context of APC gene transfer. Thus, we describe  
13 the synthesis and characterization of a second-generation mannosylated poly(beta-amino ester)  
14 library stratified by molecular weight. To better understand the APC-specific structure-function  
15 relationships governing polymeric gene delivery, the library was systematically characterized by  
16 (1) polymer molecular weight, (2) relative mannose content, (3) polyplex biophysical properties,  
17 and (4) gene delivery efficacy. In this library, polymers with the lowest molecular weight and  
18 highest relative mannose content possessed gene delivery transfection efficiencies as good as or  
19 better than commercial controls. Among this group, the most effective polymers formed the  
20 smallest polymer-plasmid DNA complexes (~300 nm) with moderate charge densities (<10 mV).  
21 This convergence in polymer structure and polyplex biophysical properties suggests a unique  
22 mode of action and provides a framework within which future APC-targeting polymers can be  
23 designed.  
24  
25  
26  
27  
28  
29  
30  
31  
32  
33  
34  
35  
36  
37  
38  
39  
40  
41  
42  
43  
44  
45  
46  
47  
48  
49  
50  
51  
52  
53  
54  
55  
56  
57  
58  
59  
60

## INTRODUCTION

Gene delivery is a therapeutic treatment that is defined as the transport of recombinant genetic material (DNA and/or RNA) into target cells for the eventual modulation of host cell expression patterns. This form of treatment has been commercially applied to combat cancer or restore deficient enzyme activity and has been documented as a strategy for addressing notable elusive diseases (e.g., HIV).<sup>1, 2</sup> Driving the approach is the choice of delivery vector or technique, including biomaterials (polymers and lipids), biological vehicles (bacteria, viruses, and other alternatives), and physically-derived mechanisms (e.g., electroporation). Of particular interest, cationic polymers (CP) represent a viable gene delivery option due to their notable design plasticity, low cytotoxicity, and effective delivery outcomes.<sup>3-6</sup> Within this set of vectors, poly(beta-amino esters) (PBAEs) have been used extensively in the successful delivery of various genetic cargo in both *in vitro* and *in vivo* applications.<sup>7-10</sup> Current gene delivery research has predominately focused on engineering criteria towards optimal uptake and processing that is applicable for all cell types.<sup>1</sup> Designing CPs for universal cellular uptake directs polyplexes (polymer complexed to plasmid DNA [pDNA]) through generalized mechanisms that result in ubiquitous (non-specific) delivery outcomes when applied *in vivo*. Indeed, general administration can prompt powerful systemic responses that are often critical towards alleviating diseases that afflict multiple tissue/organ systems but are largely ineffective when targeting diseases that require spatially acute responses.<sup>1</sup>

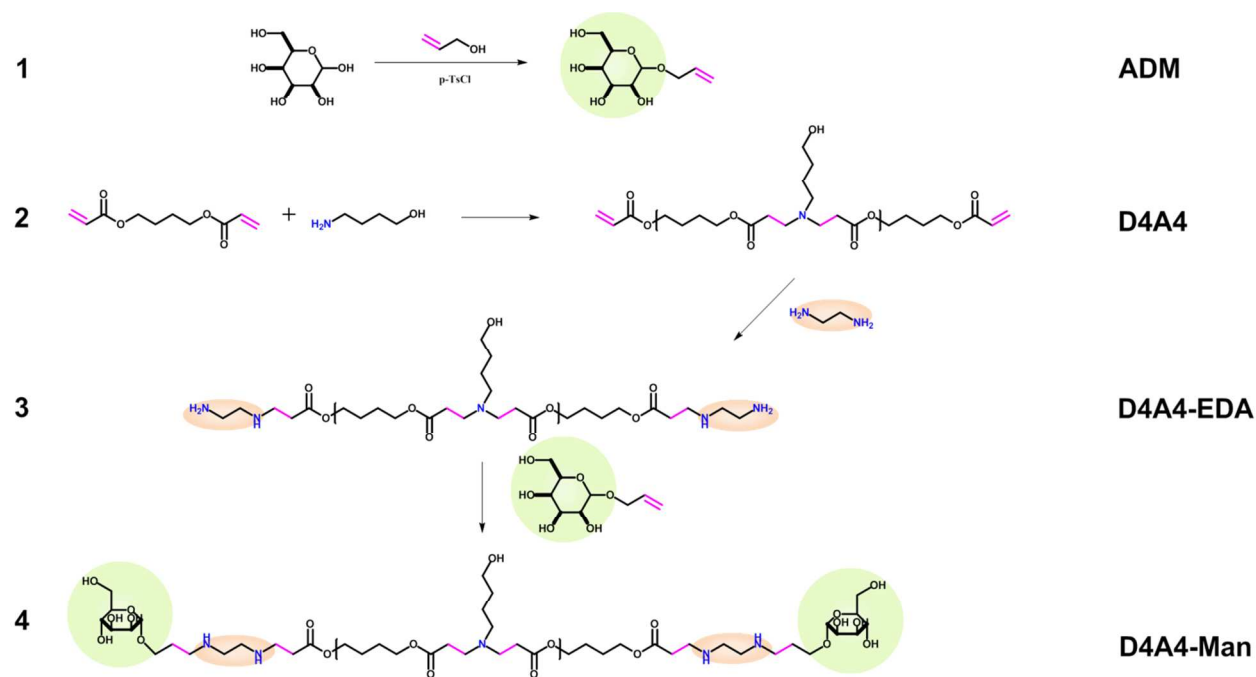
In an effort to provide cell or tissue targeting, numerous strategies have been employed that include restriction of genetic cargo activity to a desired cell type via tissue-specific promoters.<sup>11</sup> Specificity has also been achieved by engineering the PBAE component via grafting of cell-homing ligands,<sup>12</sup> tuning of the polyplex physical characteristics,<sup>13, 14</sup> or the

1  
2  
3 inclusion of stimulus-driven release.<sup>15</sup> We previously demonstrated the ability to simultaneously  
4 restrict and increase delivery to antigen presenting cells (APCs; macrophages and dendritic cells)  
5 both *in vitro* and *in vivo* via novel chemical linkage of mannose to the terminal ends of amine-  
6 capped PBAEs to serve as polymeric genetic vaccine vectors.<sup>12, 16</sup> Mannose was selected as the  
7 grafting ligand due to the upregulation of the corresponding receptor (CD206) on the surface of  
8 APCs.<sup>17</sup> CD206 is a member of the calcium-dependent lectin family that selectively recognizes  
9 polysaccharides (mannose, fucose, and N-acetylglucosamine) which are commonly present on  
10 pathogens.<sup>18</sup> In addition, previous studies have suggested that inclusion of mannose induces an  
11 alternative processing mechanism of the polyplex that is more permissive towards gene delivery  
12 and eventual production of antigenic peptides.<sup>12, 19</sup>  
13  
14  
15  
16  
17  
18  
19  
20  
21  
22  
23  
24  
25  
26  
27

28 During our initial studies using mannosylated PBAEs (PBAE-Man), a library of  
29 structurally-diverse polymers was assessed for optimal gene delivery. Due to the limited number  
30 of polymers assessed and an incomplete understanding of fundamental APC-associated vector  
31 processing steps, limited information was ascertained regarding the polymeric features governing  
32 gene delivery results. However, initial trends suggested that, contrary to the existing paradigm  
33 (as it relates to non-APCs),<sup>1, 3</sup> gene delivery was inversely correlated with molecular weight.  
34 Specifically, the lowest molecular weight polymers provided optimal gene delivery.<sup>12</sup> However,  
35 recent studies have highlighted the need for cell-specific evaluation of gene delivery vectors as  
36 structure-function relationships are not universal.<sup>20</sup>  
37  
38  
39  
40  
41  
42  
43  
44  
45  
46  
47  
48  
49

50 Given the contradictory nature of these findings, we designed the present study to analyze  
51 gene delivery outcomes by utilizing a library of stratified molecular weights of the previously  
52 identified optimally performing polymer. In so doing, statistically significant structure-function  
53 trends emerged that prompt the reconsideration of design parameters for CP-based APC gene  
54  
55  
56  
57  
58  
59  
60

delivery vectors. In addition, out of necessity to improve the throughput of fundamental polymer characterization techniques, we developed an NMR-based approach to evaluate polymer degradation profiles that significantly reduces experimental cost and instrumentation time.



**Scheme 1.** Polymer synthesis methodology for mannosylated poly( $\beta$ -amino esters). (1) Allyl- $\alpha$ -D-mannopyranoside (ADM) was synthesized as a precursory reaction. (2) Diacrylate and amine monomers were co-polymerized to synthesize acrylate-terminated polymers (D4A4) that were then (3) amine-capped using an excess of ethylenediamine. (4) Amine-capped D4A4 (D4A4-EDA) molecules were then reacted with ADM to yield mannosylated polymers.

## MATERIALS AND METHODS

**Measurements.** All  $^1\text{H-NMR}$  spectra were measured at 500 MHz in  $d$ -DMSO using a Varian INOVA-500 spectrometer maintained at 25°C with tetramethylsilane (TMS) as an internal reference standard. GPC data were acquired from a Viscotek system equipped with a

1  
2  
3 VE-3580 refractive index (RI) detector, a VE 1122 pump, and two mixed-bed organic columns  
4 (PAS-103M and PAS-105M). Dimethylformamide (DMF; HPLC) containing 0.01 M LiBr was  
5 used as a mobile phase with a flow rate of 0.5 mL/min at 55°C. The GPC instrument was  
6 calibrated through narrowly-dispersed linear polystyrene standards purchased from Varian.  
7  
8 Average hydrodynamic diameters ( $D_h$ ) and zeta potential of polyplexes were obtained using DLS  
9 on a Zetasizer nano-ZS90 (Malvern, Inc.) at 25°C. All experiments were conducted using a 4  
10 mW 633 nm HeNe laser as the light source at a fixed measuring angle of 90° to the incident laser  
11 beam. The correlation decay functions were analyzed by cumulants method coupled with Mie  
12 theory to obtain volume distribution. Microplate experiments were analyzed using a Synergy 4  
13 Multi-Mode Microplate Reader (BioTek Instruments, Inc.). FACS analysis was conducted using  
14 a Calibur flow cytometer (Becton Dickinson, Franklin Lakes, NJ).  
15  
16  
17  
18  
19  
20  
21  
22  
23  
24  
25  
26  
27  
28  
29

30 **Materials.** Monomers were purchased from Sigma-Aldrich (St. Louis, MO). Acetone  
31 (HPLC), DMF (HPLC), DMSO ( $\geq 99.7\%$ ), heat inactivated FBS, MEM sodium pyruvate,  
32 HEPES buffer, penicillin/streptomycin solution, D-(+)-glucose, and RPMI-1640 were purchased  
33 from Fisher Scientific (Pittsburgh, PA). Allyl alcohol ( $\geq 99\%$ ), D-(+)-mannose (cell culture  
34 grade) and 4-toluenesulfonyl chloride (p-TsCl) were purchased from Sigma-Aldrich (St. Louis,  
35 MO). Phosphate buffered saline (PBS) and 3 M sodium acetate (NaOAc) were purchased from  
36 Life Technologies (Grand Island, NY).  
37  
38  
39  
40  
41  
42  
43  
44  
45  
46  
47

48 **Synthesis of Allyl- $\alpha$ -D-mannopyranoside (ADM).** ADM was synthesized by dissolving  
49 3 g of D-(+)-mannose and 18 mg p-TsCl in allyl alcohol (20 mL) at 90°C under reflux for 24 h.  
50 The resulting reaction solution was concentrated by vacuum distillation at 35°C.  
51  
52  
53  
54  
55  
56  
57  
58  
59  
60

1  
2  
3       **Synthesis of Mannosylated Poly(beta-amino esters).** Mannosylated-PBAEs (PBAE-  
4 Man) were generated as before<sup>12, 16</sup> except acrylate-terminated PBAEs were synthesized using a  
5 modified previous protocol<sup>20</sup> in DMSO at fourteen different amine/diacrylate molar ratios (using  
6 1,000 mg amine) for 5 days at 60°C (Schematic 1). Variance of molar ratios permitted tunable  
7 control of the base polymer molecular weight (Table 1). Acrylate-terminated polymers were  
8 then reacted with excess ethylenediamine to amine-cap the terminal ends. Specifically, acrylate-  
9 terminated polymers were dissolved in DMSO at 167 mg/mL and reacted with 5 M  
10 ethylenediamine (in DMSO) at room temperature for 24 h. Amine-capped polymers were  
11 purified by dialysis followed by evaporation under vacuum. Dialysis procedures were conducted  
12 against acetone using molecular porous membrane tubing (Spectra/Por Dialysis Membrane,  
13 Spectrum Laboratories Inc.) with an approximate molecular weight cut off at 3,500 Da. Amine-  
14 capped PBAEs were then reacted with ADM at a 1:2 molar ratio in DMSO at 90°C for 24 h and  
15 then purified via dialysis as before. Structure and purity of polymers were confirmed using <sup>1</sup>H  
16 NMR spectroscopy.

17  
18  
19       **Degradation Studies.** Desiccated PBAE samples were resuspended to a concentration of  
20 20 mg/mL. RPMI-1640 (pH 7.4) and 25 mM NaOAc buffer (pH 5.15) with 50% FBS were used  
21 as the suspension media. Alternatively, for some samples, water (pH 7.4) was used as the  
22 suspension medium. Solutions were sealed in glass vials and incubated at 37°C with mild  
23 shaking. At predefined time intervals, aliquots of 0.5 mL of polymer solution were withdrawn  
24 and fully dried under vacuum. The resulting polymer was dissolved in d-DMSO for <sup>1</sup>H-NMR  
25 analysis.

26  
27  
28       To perform degradation studies in various buffers, <sup>1</sup>H NMR spectroscopy was utilized to  
29 calculate the relative hydroxyl group generation based on the resonance intensities of the OH  
30  
31  
32

1  
2  
3 protons of the degradants at 4.2-4.5 ppm relative to the 12  $CH_2$  protons at 3.95-4.05, 2.6-2.7, and  
4  
5 1.3-1.4 ppm of the undegraded polymer (Index). This value was then analyzed to yield a relative  
6  
7 degradation metric, which has been termed the Relative Hydroxyl Group Increase (RHGI).  
8  
9

10  
11 RHGI was calculated by:

$$12 \quad 13 \quad 14 \quad 15 \quad 16 \quad 17 \quad 18 \quad 19 \quad 20 \quad 21 \quad 22 \quad 23 \quad 24 \quad 25 \quad 26 \quad 27 \quad 28 \quad 29 \quad 30 \quad 31 \quad 32 \quad 33 \quad 34 \quad 35 \quad 36 \quad 37 \quad 38 \quad 39 \quad 40 \quad 41 \quad 42 \quad 43 \quad 44 \quad 45 \quad 46 \quad 47 \quad 48 \quad 49 \quad 50 \quad 51 \quad 52 \quad 53 \quad 54 \quad 55 \quad 56 \quad 57 \quad 58 \quad 59 \quad 60$$
$$RHGI = \frac{OH}{Index} - H$$

Hydroxyl group from the degradation resultant:

$$OH = I_{(4.5-4.2)}$$

Methylene groups (as a reference of hydrogen amount) from the degradation resultant:

$$H = (I_{(4.05-3.95)} + I_{(2.7-2.6)} + I_{(1.4-1.3)})/12$$

Index from the original un-degraded polymer:

$$Index = \frac{I_{(4.5-4.2)}}{(I_{(4.05-3.95)} + I_{(2.7-2.6)} + I_{(1.4-1.3)})/12}$$

Degradation for each polymer was determined by linear regression using the RHGI value of the 7<sup>th</sup> day divided by two as the as respective half-life value. For example, P14 in RPMI with serum has a 7<sup>th</sup> day RGHI value of 2.3 (SI NMR Degradation Data Set), which when halved is 1.15. Using regression analysis and other RGHI values, the half-life is approximately 8 h. For comparison to established techniques, degradation samples prepared and processed as described above were withdrawn and fully dried under vacuum, and each resulting polymer sample was dissolved in DMF for GPC analysis (Figure S1).

1  
2  
3  
4       **Preparation of Polymer:pDNA Polyplexes.** Polyplexes were prepared by electrostatic  
5 interaction between respective PBAEs and pDNA by mixing three different weight ratios (50:1,  
6 100:1, and 200:1) of polymer to 500 ng of pDNA. First, working dilutions of PBAEs were  
7 prepared in 25 mM NaOAc (pH 5.15) to a final concentration of 4 mg/mL. Depending on the  
8 desired weight ratio, differing amounts of PBAE stock solution were mixed with pDNA in 25  
9 mM NaOAc (pH 5.15), gently vortexed, and incubated for 30 min. Taking a 200:1 polyplex as  
10 an example, 125  $\mu$ L of PBAE stock solution was mixed with 2,500 ng pDNA and 25 mM  
11 NaOAc (pH 5.15), as needed, to provide a final volume of 150  $\mu$ L, which was then distributed as  
12 500 ng pDNA/well.  
13  
14  
15  
16  
17  
18  
19  
20  
21  
22  
23  
24

25       **Polyplex Characterization.** Using polyplexes prepared as described above, zeta  
26 potential and effective diameter were measured in either PBS (pH 7.4) or 25 mM NaOAc (pH  
27 5.15). To assess polyplex serum stability via monitoring particle diameter changes over time,  
28 200:1 polyplexes were incubated in either PBS (pH 7.4) or 25 mM NaOAc (pH 5.15) that each  
29 contained 50% v/v FBS. Polyplexes were analyzed for effective diameters monitored every 15  
30 minutes and these values were then standardized by their respective serum-free diameter. All  
31 data points result from three independently formulated polyplex samples measured five times per  
32 sample.  
33  
34  
35  
36  
37  
38  
39  
40  
41  
42  
43  
44

45       **Gene Delivery Assessments.** For gene delivery experiments, a RAW264.7 cell line  
46 (kindly provided by Dr. Terry Connell, Department of Microbiology and Immunology,  
47 University at Buffalo) was cultured in growth medium (50 mL of FBS (heat inactivated), 5 mL  
48 of 100 mM MEM sodium pyruvate, 5 mL of 1 M HEPES buffer, 5 mL of penicillin/streptomycin  
49 solution, and 1.25 g of D-(+)-glucose added to 500 mL RPMI-1640 and filter sterilized) in T75  
50 flasks at 37°C/5% CO<sub>2</sub> prior to seeding at a density of  $3 \times 10^4$  cells/well in clear, tissue culture-  
51  
52  
53  
54  
55  
56  
57  
58  
59  
60

1  
2  
3 treated, sterile, polystyrene 96-well plates in 100  $\mu$ L growth medium/well and allowed 24 h for  
4 attachment. Following the 24 h incubation, the original medium was removed and replaced with  
5  
6 100  $\mu$ L fresh growth medium plus 30  $\mu$ L of PBAE:pDNA polyplexes, prepared as described  
7  
8 above (total volume of 130  $\mu$ L), and incubated for an additional 4 h. Polyplex-containing media  
9  
10 was then removed using a 12-channel aspirating wand and replaced with 100  $\mu$ L fresh,  
11  
12 antibiotic-free growth medium preheated to 36°C. After 48 h (72 h after initial seeding), plates  
13  
14 were analyzed for transfection efficiency using flow cytometry. To conduct flow cytometry  
15  
16 assessment, cells were first washed with ice-cold PBS and detached from the well surface using  
17  
18 cell scrapers. The fraction of EGFP-expressing cells was quantified using gating based upon  
19  
20 transfections using pDNA not encoding EGFP (negative control). Commercial controls,  
21  
22 FuGENE HD, Xfect, and JET-PEI were utilized according to different manufacturer's  
23  
24 instructions. Results derive from four independent experiments and twelve replicates per  
25  
26 experiment.  
27  
28  
29  
30  
31  
32  
33  
34

35 To determine if transfection was affected by the presence of free mannose and  
36  
37 physiological levels of serum, polyplexes were prepared at a 200:1 PBAE-to-pDNA weight ratio.  
38  
39 Vectors were then transfected as before with the following alterations. Prior to transfection, cell  
40  
41 media was replaced with growth medium containing 1 mM mannose or with 50% v/v FBS,  
42  
43 incubated 30 minutes, and transfected as before. After the 4 h transfection incubation, the altered  
44  
45 media was replaced with regular growth media and assessed for gene delivery as described  
46  
47 above.  
48  
49  
50  
51

52 Mannose and serum sensitivities of gene delivery (as described in the main text) were  
53  
54 calculated using the following formula:  
55  
56  
57  
58  
59  
60

$$\text{Sensitivity} = \frac{\text{GD} - \text{IGD}}{\text{GD}}$$

Where, GD = Uninhibited Gene Delivery and IGD = Inhibited Gene Delivery

**Statistical Analysis.** Unless otherwise indicated, data presented were generated from three independent experiments. Error bars represent standard deviation values. All statistical significance comparisons between groups were performed using a one-way ANOVA with Dunnett (to compare within groups) post-tests.

## RESULTS AND DISCUSSION

**Polymer Synthesis and Characterization.** Polymers were synthesized using our recently developed mannose end-capping strategy (Scheme 1).<sup>12</sup> However, unlike before, the ratio of diacrylate to amine monomers (D:A ratio) used in the synthesis of the base polymer (Scheme 1, Step 2) was systematically varied. Variation of the D:A ratio was used to generate stratified molecular weight polymers with the same chemical background. Each respective PBAE structure and purity was confirmed using <sup>1</sup>H NMR (Table 1). Gel permeation chromatography (GPC) and dynamic light scattering (DLS) were used to measure molecular weight, polydispersity index (PDI), and zeta potential (in two buffers) of the polymers (Table 1; Figure 1A). The generated polymer library spanned a molecular weight (weighted) range from 6.8 to 33.7 kDa with PDI values (~1.4-2.5) characteristic of PBAEs. Furthermore, zeta potential values of the polymer library increased with increasing molecular weight regardless of buffer (Figure 1B and C).

**Table 1.** Polymer Synthesis and Characterization.

Polymer	D:A Ratio	PDI <sup>GPC</sup>	M <sub>n</sub> <sup>GPC</sup> (Da)	M <sub>w</sub> <sup>GPC</sup> (Da)	Zeta Potential (mV) PBS (pH 7.4)	Zeta Potential (mV) NaOAc (pH 5.15)
---------	-----------	--------------------	------------------------------------	------------------------------------	----------------------------------	-------------------------------------

P1	1.025	2.477	13,623	33,745	-8.6	32.6
P2	1.0375	1.641	13,425	22,031	-5.3	34.0
P3	1.05	1.536	11,961	18,372	-6.2	33.6
P4	1.0625	1.370	11,848	16,232	-8.3	32.4
P5	1.075	1.629	10,474	17,063	-7.7	32.7
P6	1.1	1.642	10,130	16,633	-8.8	34.6
P7	1.125	1.833	7,902	14,484	-8.0	31.9
P8	1.15	1.468	7,312	10,734	-11.1	27.5
P9	1.175	1.699	6,589	11,195	-12.1	28.6
P10	1.2	1.549	5,966	9,241	-11.2	24.9
P11	1.225	1.590	5,510	8,761	-11.4	26.4
P12	1.25	1.600	5,112	8,180	-12.7	24.0
P13	1.275	1.638	4,673	7,654	-12.9	20.9
P14	1.3	1.615	4,479	7,234	-11.2	21.4

**Polymer Degradation Studies.** A prerequisite for the translational usage of biomaterial-based delivery vectors is the successful demonstration of a balanced degradation profile. In particular, the degradation profiles of CPs play a critical role in predicting potential circulation residency time, genetic cargo unpackaging, gene delivery efficiency, and vector-associated cytotoxicity.<sup>1</sup> Premature degradation profiles, for example, indicate potential fragility of polyplexes; whereas, extended stability may result in the inability to unpackage cargo in addition to increased cytotoxicity.<sup>1, 3, 21</sup> Previously, we developed methodology that more accurately assessed degradation profiles in media that mimicked physiologically-relevant settings.<sup>12</sup> Specifically, polymers were incubated for various time points in water (pH 7.4; traditional degradation buffer) or either RPMI (pH 7.4; mimics the circulation/extracellular environment) or 25 mM NaOAc (pH 5.15; mimics the lysosome) with and without serum. However, a limitation of the previous technique was the reliance on GPC, which introduced time and cost constraints. For example, use of GPC for degradation studies requires regimented sample preparation, an

hour instrumentation time per sample, and is not able to distinguish false positives or failures (usually due to contamination).

**Table 2.** Polymer Degradation in Various Buffers.

Polymer	Half-life (h)	
	RPMI w/ Serum (pH 7.4)	25 mM NaOAc w/ Serum (pH 5.15)
P1	4	4
P2	5	4
P3	3	5
P4	6	4
P5	4	3
P6	7	4
P7	5	4
P8	8	4
P9	6	7
P10	9	4
P11	6	4
P12	5	4
P13	4	4
P14	8	8

1  
2  
3  
4 Taking into account the limitations of the previous methodology, we developed an NMR-  
5 based alternative that significantly reduces time- and cost-demands of degradation studies. In  
6 doing so, a new variable (Relative Hydroxyl Group Increase [RHGI]) was developed and used in  
7 the context of physiological-relevant buffers to calculate the relative half-life of each polymer  
8 (Table 2). The results indicate that degradation was independent of molecular weight and  
9 primarily influenced by buffer pH.  
10  
11  
12  
13  
14  
15  
16  
17  
18  
19

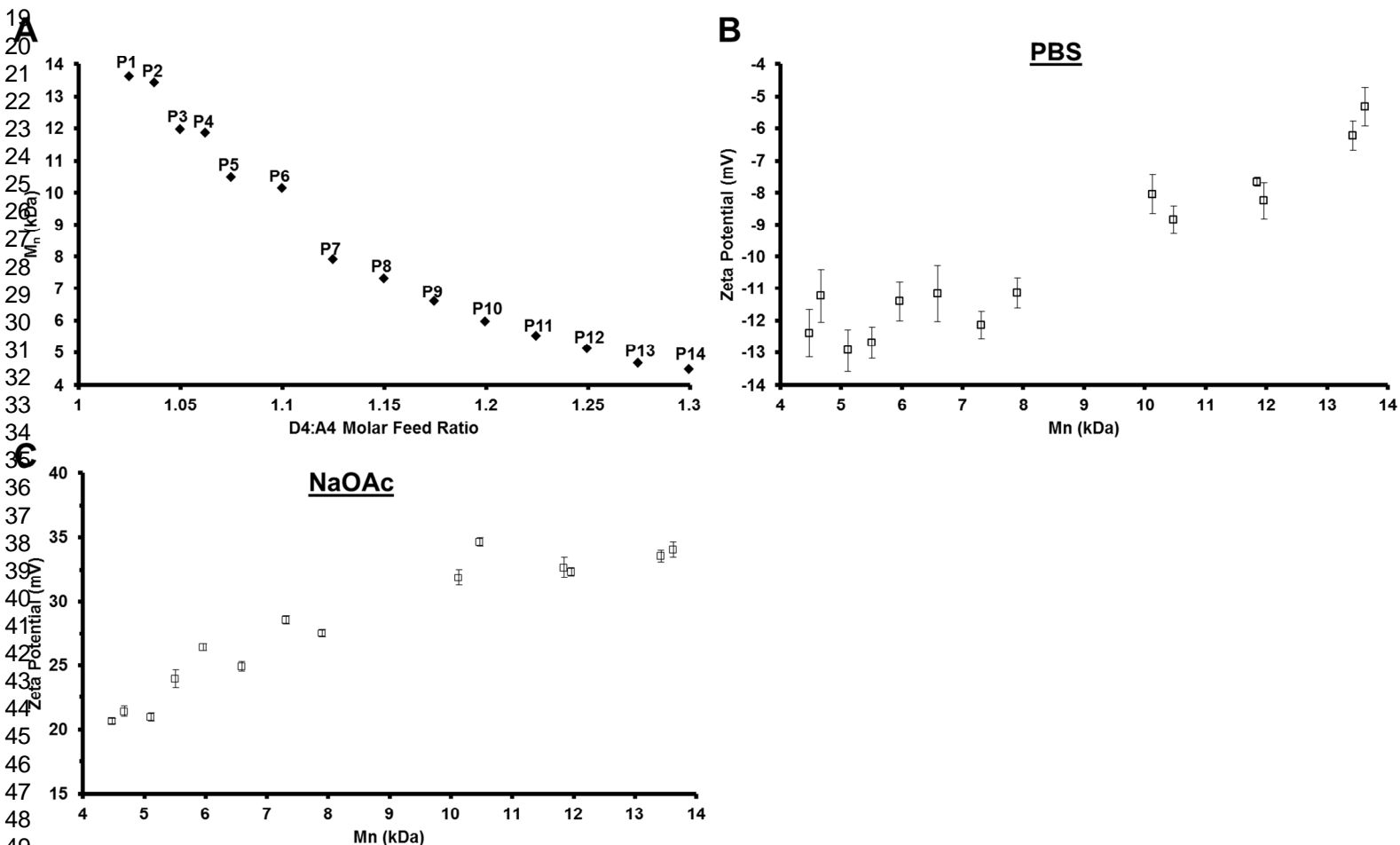
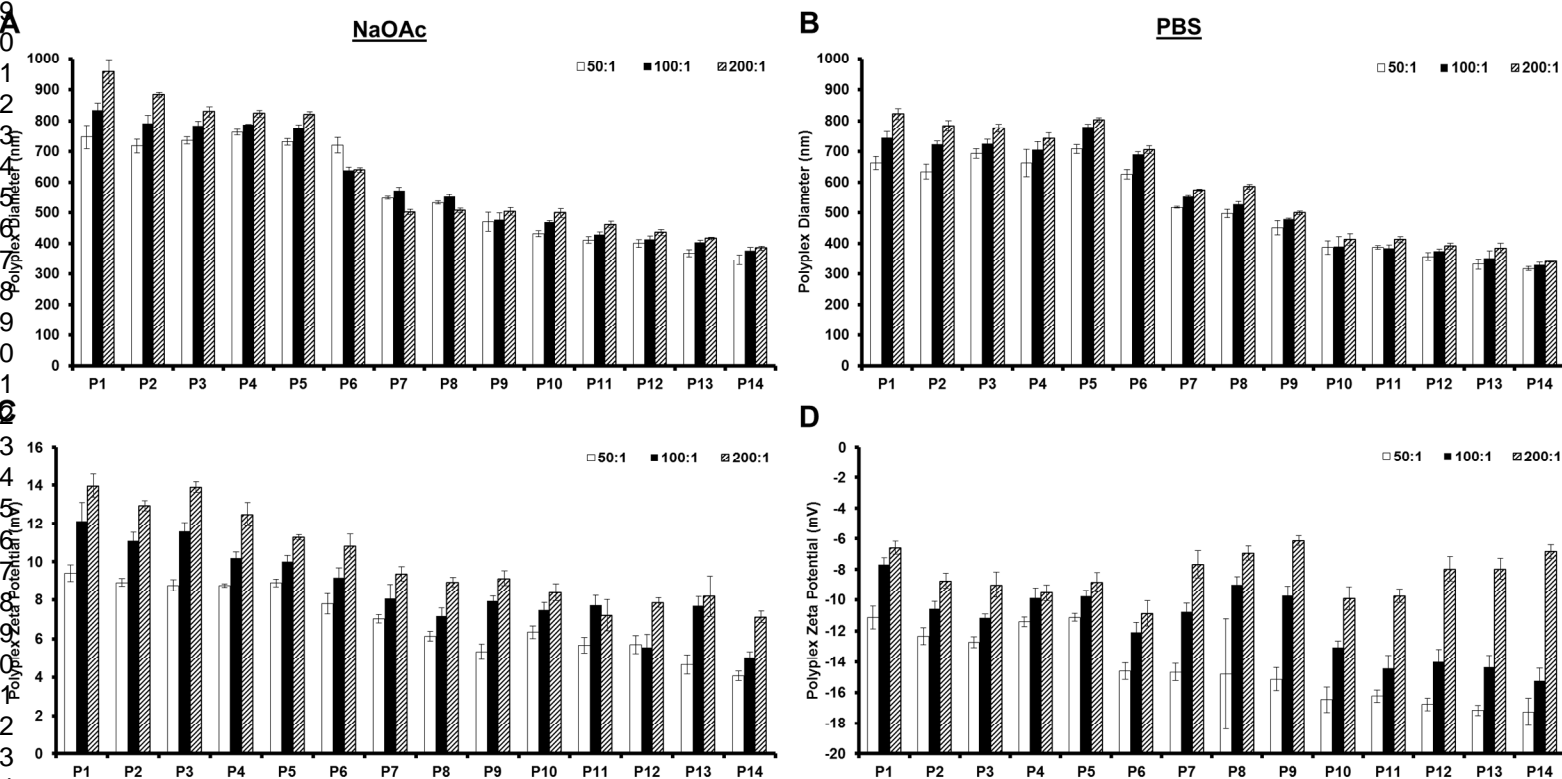


**Figure 1.** Polymer characterization data. (A) Numbered polymer molecular weight as a function of diacrylate (D4) to amine (A4) monomer feed ratios. Data points have been labeled with the associated polymer name. Zeta potential measurements in either PBS (B) or 25 mM NaOAc (C) relative to numbered polymer molecular weight.

Utilization of the RGHI methodology provides numerous advantages and opportunities for time- and cost-reductions (Figure S1). Specifically, using our 140 polymer samples (14 polymers  $\times$  5 time points  $\times$  2 buffers = 140) as an example, the traditional GPC method requires 140 h (1 h/sample) and \$2,800 (\$20/sample [University at Buffalo Instrumentation quote]). In comparison, using the RGHI method reduces these requirements to 12 h and \$700 and provides time and cost reductions that range from 12-18 $\times$  and 2-4 $\times$ , respectively.

**Polyplex Preparation and Characterization.** To form polyplexes, three polymer:pDNA weight ratios were selected based upon our previous report.<sup>12</sup> Specifically, 50:1, 100:1, and 200:1 were used in initial gene delivery experiments; whereas, only 200:1 was used during inhibition and structure-function studies (to be described later).



1  
2  
3 **Figure 2.** Characterization summary of D4A4-Man polyplexes. Polyplex diameter (A & B) and  
4 zeta potential (C & D) in 25 mM NaOAc (left panels) or PBS (right panels). All panel B values  
5 were significantly lower (95% confidence) than corresponding values in panel A.  
6  
7

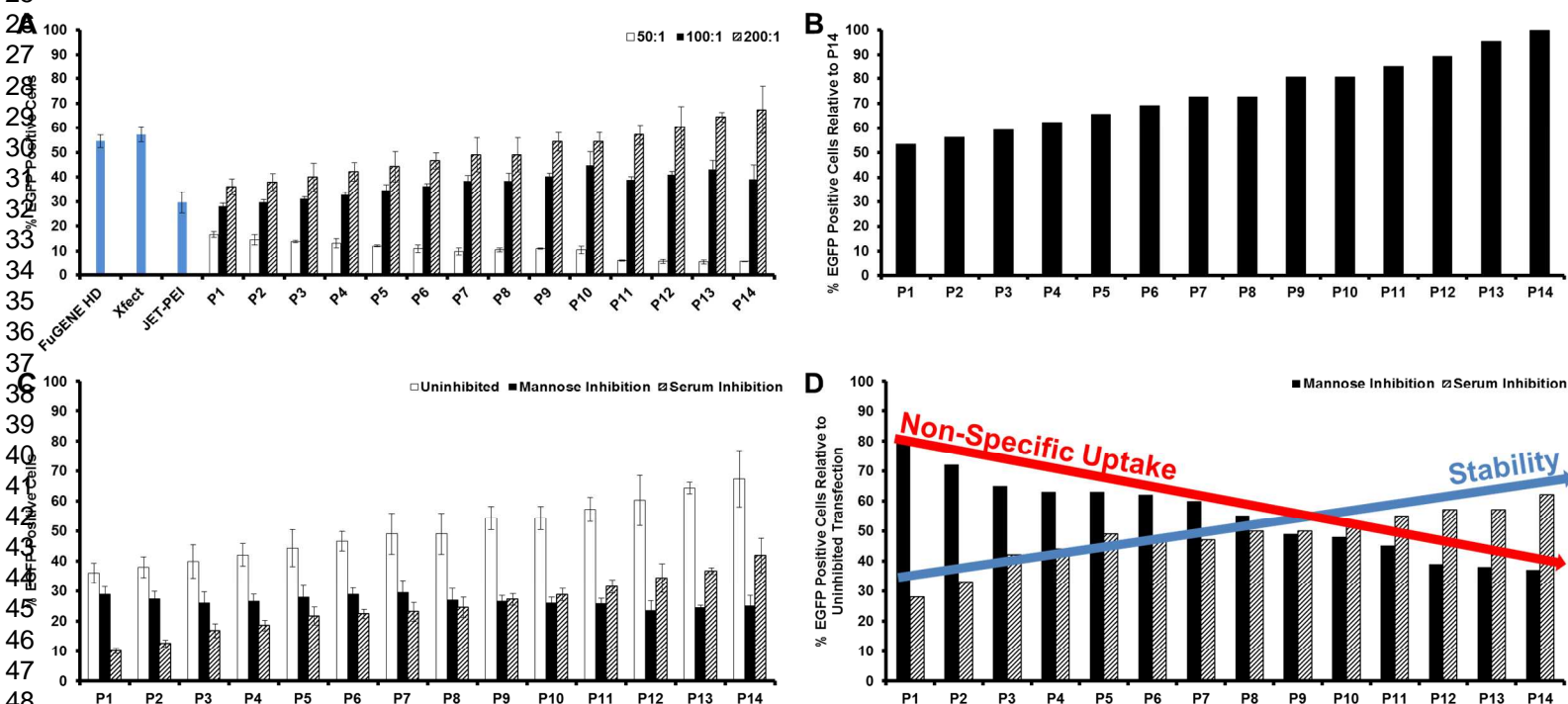
8  
9  
10 To assess the biophysical properties associated with polyplexes, DLS was used to  
11 measure the particle effective diameter and zeta potential in both 25 mM NaOAc and PBS  
12 (Figure 2). Polyplexes ranged in size from 300-1,000 nm, increasing with higher molecular  
13 weights and (in most cases) polymer:pDNA weight ratios. Neutral pH conditions (PBS)  
14 prompted statistically significant tighter condensation of polyplexes (Figure 2B), presumably due  
15 to the lack of excessive protonation (which may promote aggregation<sup>1,3</sup>) and neutralization of all  
16 remaining charges by bound pDNA. Furthermore, polymer molecular weight was linearly  
17 correlated with increasing polyplex zeta potential and polyplex size (Figure S2A). In addition,  
18 for each unit molecular weight required to complex pDNA, there is a linear increase in mannose  
19 content (each individual polymer chain is capped with two mannose molecules) that may further  
20 influence condensation and zeta potential of polyplexes. When relative mannose content is taken  
21 into account, higher mannose content (associated with smaller polymer chains) also leads to  
22 reduced zeta potential and polyplex diameter values (Figure S2B).  
23  
24  
25  
26  
27  
28  
29  
30  
31  
32  
33  
34  
35  
36  
37  
38  
39

40  
41 As a last form of assessment, polyplexes were prepared as described above, incubated in  
42 physiologically-relevant media, and monitored for changes in relative diameter over time to  
43 determine polyplex stability (Figure S3). Upon incubation in 25 mM NaOAc containing 50%  
44 v/v serum (Figure S3A), relative polyplex diameters increased with respect to time for most  
45 polymers. The upper-half molecular weight polymers (P1-P7) displayed the largest relative  
46 changes in polyplex diameter. This observation presumably is the result of excessive protonation  
47 which may mediate non-specific serum deposition or polyplex aggregation. Conversely, the  
48  
49  
50  
51  
52  
53  
54  
55  
56  
57  
58  
59  
60

1  
2  
3 lower-half molecular weight polymers (with exception to P8 and P10) did not display any  
4 appreciable changes in diameter over time. Upon incubation in PBS containing 50% v/v serum  
5 (Figure S3B), only P1 and P7 demonstrated changes in polyplex diameter. All other polymers  
6 mediated the formation of smaller polyplexes. This may be the result of a shielding effect  
7 conferred by the attachment of mannose combined with increased colloidal pressure (derived  
8 from increased negatively-charged serum) driving the compaction of polyplexes.  
9  
10  
11  
12  
13  
14  
15  
16

17 **Gene Delivery Studies.** Previously, we identified that mannosylation (either by  
18 chemical grafting or free addition) positively affected gene delivery in direct response to binding  
19 and processing through a CD206-dependent mechanism.<sup>12</sup> However, despite successful  
20 transfection data, clear molecular weight trends were not observed due to the narrow range of  
21 molecular weights evaluated. Thus, the purpose of the present study is the systematic analysis of  
22 molecular weight upon APC-mediated gene delivery. Furthermore, polyplexes formed using  
23 three polymer:pDNA ratios were compared to select commercial controls (representing distinct  
24 categories of gene delivery vectors – lipid-based [FuGENE HD], unmodified CP [Xfect],  
25 mannosylated CP [JET-PEI]) during gene delivery to a murine macrophage cell line known to  
26 express CD206 (Figure 3).<sup>22-24</sup> Transfection efficiency of polyplexes was found to correlate  
27 positively with increasing polymer:pDNA ratios (Figure 3A). Unexpectedly, for the highest  
28 polymer:pDNA ratio, gene delivery increased linearly with decreasing polymer molecular  
29 weight; the lowest molecular weight polymer (P14) mediated the highest gene delivery at a 200:1  
30 ratio (Figure 3A and B). This finding is interesting because it is commonly accepted that higher  
31 molecular weight polymers mediate the highest gene delivery.<sup>1</sup> However, previous studies were  
32 not applied to APCs, which are noted for their unique processing of external cargo.<sup>12</sup>  
33  
34  
35  
36  
37  
38  
39  
40  
41  
42  
43  
44  
45  
46  
47  
48  
49  
50  
51  
52  
53  
54  
55  
56  
57  
58  
59  
60 Accordingly, it is possible that the mannose-mediated uptake directs polyplexes toward

1  
2  
3 endocytic mechanisms that are more permissive to gene delivery by lower molecular weight  
4 polymers. Alternatively, gene delivery improvements may be explained by a size-exclusion  
5 effect. Specifically, polyplexes larger than 500 nm are biased for phagocytosis-mediated uptake,  
6 which is known to be more degradative and less prone to phagosomal escape.<sup>4, 5</sup> At the lowest  
7 polymer:pDNA ratio (50:1), gene delivery is negatively correlated with decreasing molecular  
8 weight (Figure 3A). Presumably, this occurs because lower molecular weight polymers do not  
9 effectively condense pDNA at lower weight ratios, which results in increased fragility and  
10 degradation of the associated polyplexes. Thus, taking into account the optimal levels of gene  
11 delivery, 200:1 polyplexes were selected for subsequent gene delivery experiments.  
12  
13  
14  
15  
16  
17  
18  
19  
20  
21  
22  
23  
24  
25



26  
27  
28  
29  
30  
31  
32  
33  
34  
35  
36  
37  
38  
39  
40  
41  
42  
43  
44  
45  
46  
47  
48  
49 **Figure 3.** Gene delivery summary. (A) Transfection efficiency (% EGFP Positive Cells) of  
50 commercial controls and D4A4-Man polyplexes at three different polymer-to-pDNA weight  
51 ratios. (B) Standardization of 200:1 transfection efficiency by top performing D4A4-Man (P14)  
52 variant. (C) Evaluation of mannose (1,000  $\mu$ M) and serum (50% v/v) inhibition of 200:1  
53  
54  
55  
56  
57  
58  
59  
60

1  
2  
3 polyplexes gene delivery efficiency. (D) Standardization of inhibited gene delivery with  
4 uninhibited values from (C). Colored arrows were added to help visualize the connection of the  
5  
6 data to expected vector properties.  
7  
8  
9

10  
11 For PBAE-Man polyplexes to be successful in translational applications, gene delivery  
12 vectors must overcome the barriers present during circulation. Key gene delivery limitations  
13 include target specificity and the documented loss-of-activity in the presence of heightened  
14 levels of extracellular protein.<sup>1</sup> These specific limitations result in significant off-target effects  
15 and premature aggregation, degradation, and clearance.<sup>3, 25</sup> As such, transfection was conducted  
16 using 200:1 polyplexes in the presence a CD206-inhibiting concentration of free mannose and a  
17 physiologically-relevant level of serum (Figure 3C). All polyplexes exhibited significant (95%  
18 confidence) drops to both mannose and serum inhibitions. However, decreasing molecular  
19 weight resulted in the formation of polyplexes that were increasingly sensitive to mannose  
20 inhibition and decreasingly sensitive to serum inhibition. To better assess the capabilities of the  
21 polyplexes, inhibition values were standardized by their respective uninhibited gene delivery  
22 capabilities (Figure 3D). These findings demonstrate that the lower molecular weight polyplexes  
23 possess the highest specificity and stability. Moreover, these results support previous studies  
24 that demonstrated increased PBAE molecular weight does not always improve transfection.<sup>26, 27</sup>  
25  
26 Collectively, these results suggest translational APC-targeting gene delivery polymers should be  
27 designed towards moderately charged and lower molecular weight alternatives.  
28  
29  
30  
31  
32  
33  
34  
35  
36  
37  
38  
39  
40  
41  
42  
43  
44  
45  
46  
47  
48  
49  
50  
51  
52  
53  
54  
55  
56  
57  
58  
59  
60

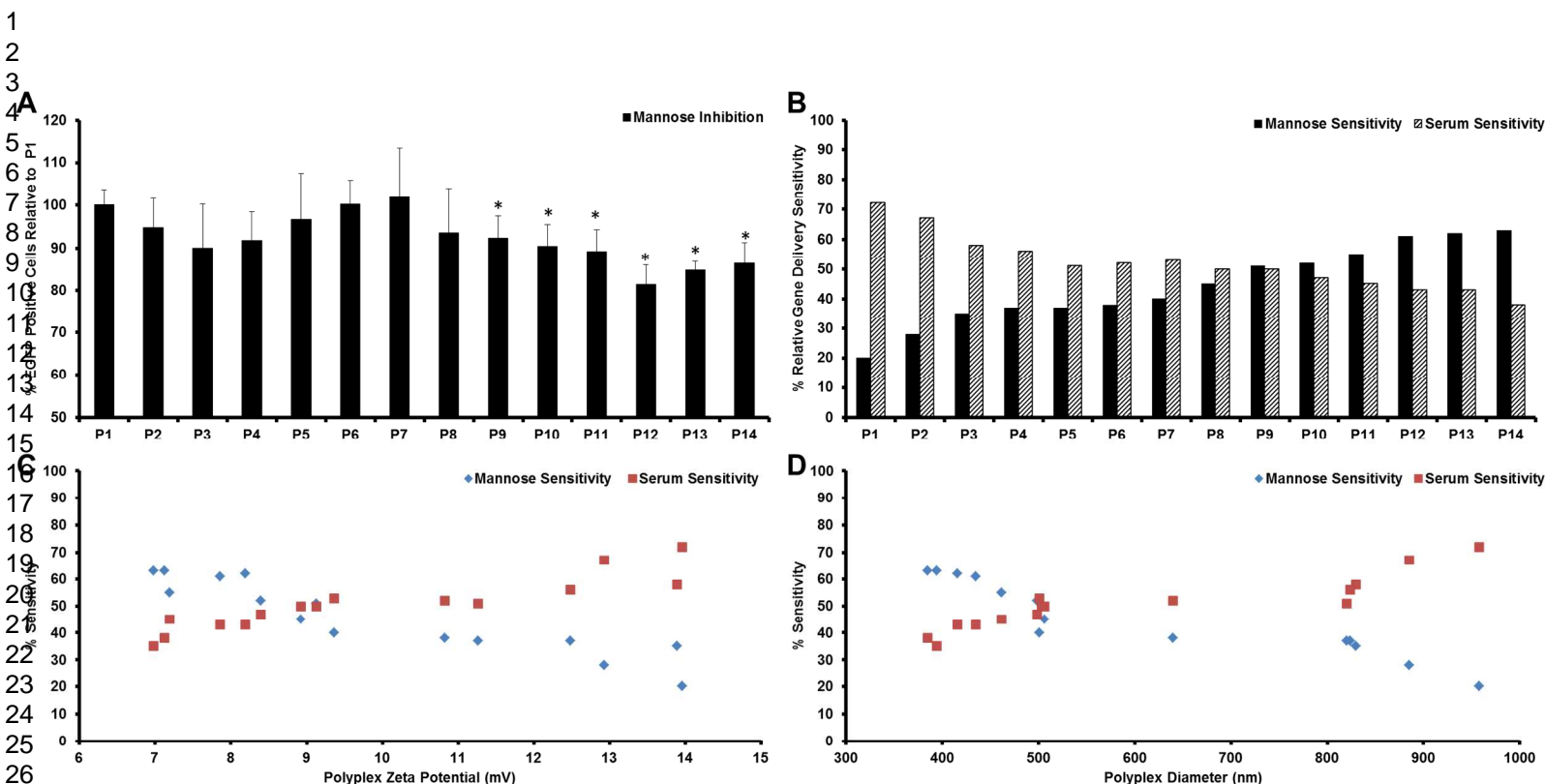


**Figure 4.** Structure-function relationships of 200:1 polyplexes. (A) Mannose-inhibited transfection efficiencies for polymers P1-P14 standardized by P1 transfection values. Total % gene delivery sensitivity (B) as a function of polyplex zeta potential (C) and diameter (D) in 25 mM NaOAc (Ph 5.15). \*Indicates statistical decrease (95% confidence) between samples compared to P1.

**Structure-function Relationships.** During the initial steps of gene delivery, vector design and polyplex biophysical characteristics significantly influence the eventual outcome. First, mannose-grafting is a potent strategy toward improving gene delivery outcomes in APCs. Due to the complexity of polymer design, however, it is often difficult to identify the influence of targeting agents (i.e., mannosylation) from various polymer chemical properties. Our current experimental plan introduces the same chemical background to each polymer and, therefore, allows direct comparison of parameters such as polymer molecular weight, polyplex zeta potential and diameter, and mannosylation. Furthermore, given the size range of the polyplexes

1  
2  
3 prepared in the current study (i.e.,  $> \sim 400 \mu\text{m}$ ), internalization and processing is primarily  
4  
5 restricted to phagocytic mechanisms.<sup>4, 5, 28, 29</sup>  
6  
7

8  
9 Polyplex zeta potential and size (diameter) are two critical properties mediating uptake,  
10  
11 endosomal release, and subsequent gene delivery (Figure S4). Specifically, uninhibited gene  
12  
13 delivery was negatively correlated with increasing polyplex zeta potential and diameter. In  
14  
15 addition, there was not a statistical dependence of gene delivery upon charge or size in the  
16  
17 presence of inhibiting concentrations of mannose; whereas, in physiological levels of serum,  
18  
19 gene delivery was negatively correlated with increasing charge and size.  
20  
21  
22  
23

24 By normalizing mannose-inhibited gene delivery values with the gene delivery of the  
25  
26 highest molecular weight polymer (P1), the resulting data allow an assessment of gene delivery  
27  
28 as a function of polymer molecular weight without the influence of mannosylation (Figure 4A).  
29  
30 Moreover, without mannose-mediated improvements, the established higher molecular weight  
31  
32 paradigm is restored. Namely, gene delivery is correlated with higher molecular weight  
33  
34 polymers (which also possessed the largest polyplex diameters and zeta potential values). These  
35  
36 observations highlight the importance of biasing polyplexes towards mannose-mediated  
37  
38 processing that in turn prompts the redirection into the recycling endocytic mechanism that is  
39  
40 more permissive to gene delivery outcomes.<sup>12</sup>  
41  
42  
43  
44  
45

46 Interestingly, the relative degree of inhibition (both mannose- and serum-dependent)  
47  
48 demonstrated by each polyplex varied in a linear fashion with polymer molecular weight  
49  
50 (Figures 3C and D), thus, prompting the development of a new comparative “sensitivity” metric  
51  
52 (Figure 4B). Here, the percent change between uninhibited and inhibited gene delivery values  
53  
54 was utilized to represent the likelihood of a particular parameter to inhibit gene delivery (i.e.,  
55  
56  
57  
58  
59  
60

1  
2  
3 higher sensitivity values indicate the higher likelihood of inhibited gene delivery in the presence  
4 of that particular parameter). Accordingly, mannose sensitivity was positively correlated with  
5 decreasing molecular weight; whereas, serum sensitivity was negatively correlated with  
6 decreasing molecular weight. This phenomenon is best explained by the interplay of polyplex  
7 relative mannose content, zeta potential, and diameter (Figure 4C and D). Polymers possessing  
8 the lowest molecular weight contain the highest relative mannose content, driving the formation  
9 of increasingly smaller sized and less cationic polyplexes (Figures S2 and S5). Consequently,  
10 the resulting polyplexes have smaller surface areas, which in turn enrich the relative mannose  
11 surface density. Collectively, these results suggest that increased serum surface deposition  
12 (attributed to electrostatically-driven interactions between the residual cationic charges of the  
13 polyplex and the anionic serum proteins coupled with increasing surface area) promotes the  
14 physical coverage of mannose molecules and, thus, inhibits mannose-mediated uptake  
15 mechanisms. However, at the smallest polyplex sizes, the increased relative mannose surface  
16 density may serve a dual function in providing a shielding layer (similar to PEGylation) that  
17 simultaneously prevents serum deposition while also providing targeting capabilities.  
18  
19  
20  
21  
22  
23  
24  
25  
26  
27  
28  
29  
30  
31  
32  
33  
34  
35  
36  
37  
38

39 In our initial studies using mannosylated PBAEs, the best performing polymer  
40 background, D4A4 (used in the current study), was further analyzed in a preliminary *in vivo*  
41 DNA vaccination study.<sup>12</sup> Although both nonmannosylated and mannosylated D4A4 polymers  
42 elicited strong immune responses, only D4A4-Man was able to evoke a response statistically  
43 higher than the commercial controls. Furthermore, the structure-function analysis presented in  
44 the previous work was limited but provided a polymer chemical background basis for  
45 engineering polyplex gene delivery specific for APCs. Given the success of the initial study, the  
46 results in this work provide new *in vitro* findings that support further *in vivo* translation.  
47  
48  
49  
50  
51  
52  
53  
54  
55  
56  
57  
58  
59  
60

## CONCLUSIONS

The library of polymers developed in this study highlights the unique ability of small, moderately charged, mannosylated PBAEs to elicit statistically significant levels of gene transfections in APCs. Taken together, the study provides fundamental insight into underlying structure-function relationships for APC-targeted gene delivery while also providing a cost-effective alternative to an established polymer degradation methodology.

## ASSOCIATED CONTENT

**Supporting Information.** Additional gene delivery and structure functions are presented. In addition, NMR data is presented including an example of the polymer degradation analysis. This material is available free of charge via the Internet at <http://pubs.acs.org>.

## AUTHOR INFORMATION

### Corresponding Author

\*Corresponding authors. Department of Chemical and Biological Engineering, University at Buffalo, State University of New York, Buffalo, NY 14260-4200, USA, Phone: 716-645-1198, Fax: 716-645-3822. Email: [blainepf@buffalo.edu](mailto:blainepf@buffalo.edu).

### Author Contributions

CHJ conceptualized and designed the overall study, conducted all biological experiments, and analyzed all data. MC, AG, AR, GZ, SL, and MT conducted and analyzed data for all material-related studies. HL and CC assisted with NMR spectra analysis. The manuscript was written through contributions of all authors. All authors have given approval to the final version of the manuscript. ‡These authors contributed equally.

## Funding Sources

The authors recognize support from NIH award AI088485 (BAP), a SUNY-Buffalo Schomburg fellowship (CHJ), and two Mark Diamond Research Fund Grants (AR and MC).

## Notes

The authors declare no competing financial interest.

## REFERENCES

1. Jones, C.H., Chen, C.K., Ravikrishnan, A., Rane, S., and Pfeifer, B.A. Overcoming nonviral gene delivery barriers: perspective and future. *Mol. Pharmaceutics* 10, 4082-98, 2013.
2. Jones, C.H., Hakansson, A.P., and Pfeifer, B.A. Biomaterials at the interface of nano- and micro-scale vector-cellular interactions in genetic vaccine design. *J. Mater. Chem. B* 2, 8053-68, 2014.
3. Pack, D.W., Hoffman, A.S., Pun, S., and Stayton, P.S. Design and development of polymers for gene delivery. *Nat. Rev. Drug Discovery* 4, 581-93, 2005.
4. Jones, C.H., Chen, C.K., Jiang, M., Fang, L., Cheng, C., and Pfeifer, B.A. Synthesis of cationic polylactides with tunable charge densities as nanocarriers for effective gene delivery. *Mol. Pharmaceutics* 10, 1138-45, 2013.
5. Chen, C.K., Jones, C.H., Mistriotis, P., Yu, Y., Ma, X., Ravikrishnan, A., Jiang, M., Andreadis, S.T., Pfeifer, B.A., and Cheng, C. Poly(ethylene glycol)-*block*-cationic polylactide nanocomplexes of differing charge density for gene delivery. *Biomaterials* 34, 9688-99, 2013.
6. Chen, C.K., Law, W.C., Aalinkeel, R., Nair, B., Kopwiththaya, A., Mahajan, S.D., Reynolds, J.L., Zou, J., Schwartz, S.A., Prasad, P.N., and Cheng, C. Well-defined degradable cationic polylactide as nanocarrier for the delivery of siRNA to silence angiogenesis in prostate cancer. *Adv. Healthc Mater.* 1, 751-61, 2012.
7. Lynn, D.M., and Langer, R. Degradable Poly( $\beta$ -amino esters): synthesis, characterization, and self-assembly with plasmid dna. *J. Am. Chem. Soc.* 122, 10761-68, 2000.
8. Guerrero-Cazares, H., Tzeng, S.Y., Young, N.P., Abutaleb, A.O., Quinones-Hinojosa, A., and Green, J.J. Biodegradable polymeric nanoparticles show high efficacy and specificity at DNA delivery to human glioblastoma *in vitro* and *in vivo*. *ACS Nano* 8, 5141-53, 2014.
9. Sunshine, J.C., Sunshine, S.B., Bhutto, I., Handa, J.T., and Green, J.J. Poly(beta-amino ester)-nanoparticle mediated transfection of retinal pigment epithelial cells *in vitro* and *in vivo*. *PLOS One* 7, e37543, 2012.
10. Sunshine, J.C., Peng, D.Y., and Green, J.J. Uptake and Transfection with Polymeric Nanoparticles Are Dependent on Polymer End-Group Structure, but Largely Independent of Nanoparticle Physical and Chemical Properties. *Mol. Pharmaceutics*, 2012.
11. Franz, W.M., Rothmann, T., Frey, N., and Katus, H.A. Analysis of tissue-specific gene delivery by recombinant adenoviruses containing cardiac-specific promoters. *Cardiovascular Research* 35, 560-6, 1997.
12. Jones, C.H., Chen, M., Ravikrishnan, A., Reddinger, R., Zhang, G., Hakansson, A.P., and Pfeifer, B.A. Mannosylated poly(beta-amino esters) for targeted antigen presenting cell immune modulation. *Biomaterials* 37, 333-44, 2015.

- 1
- 2
- 3
- 4 13. Zugates, G.T., Tedford, N.C., Zumbuehl, A., Jhunjhunwala, S., Kang, C.S., Griffith, L.G.,
- 5 Lauffenburger, D.A., Langer, R., and Anderson, D.G. Gene delivery properties of end-modified
- 6 poly(beta-amino ester)s. *Bioconjug. Chem.* 18, 1887-96, 2007.
- 7 14. Zugates, G.T., Anderson, D.G., Little, S.R., Lawhorn, I.E., and Langer, R. Synthesis of poly(beta-
- 8 amino ester)s with thiol-reactive side chains for DNA delivery. *J. Am. Chem. Soc.* 128, 12726-34,
- 9 2006.
- 10 15. Yin, Q., Gao, Y., Zhang, Z., Zhang, P., and Li, Y. Bioreducible poly (beta-amino esters)/shRNA
- 11 complex nanoparticles for efficient RNA delivery. *J. Control. Release.* 151, 35-44, 2011.
- 12 16. Jones, C.H., Ravikrishnan, A., Chen, M., Reddinger, R., Kamal Ahmadi, M., Rane, S.,
- 13 Hakansson, A.P., and Pfeifer, B.A. Hybrid biosynthetic gene therapy vector development and
- 14 dual engineering capacity. *Proc. Natl. Acad. Sci. USA* 111, 12360-5, 2014.
- 15 17. Taylor, M.E. Structure and function of the macrophage mannose receptor. *Results and Problems*
- 16 *in Cell Differentiation* 33, 105-21, 2001.
- 17 18. Dasgupta, S., Bayry, J., Lacroix-Desmazes, S., and Kaveri, S.V. Human mannose receptor
- 18 (CD206) in immune response: novel insights into vaccination strategies using a humanized mouse
- 19 model. *Expert Review of Clinical Immunology* 3, 677-81, 2007.
- 20 19. Simmons, B.M., Stahl, P.D., and Russell, J.H. Mannose receptor-mediated uptake of ricin toxin
- 21 and ricin A chain by macrophages. Multiple intracellular pathways for a chain translocation. *J.*
- 22 *Biol. Chem.* 261, 7912-20, 1986.
- 23 20. Sunshine, J., Green, J.J., Mahon, K.P., Yang, F., Eltoukhy, A.A., Nguyen, D.N., Langer, R., and
- 24 Anderson, D.G. Small molecule end group of linear polymer determines cell-type gene delivery
- 25 efficacy. *Adv. Mater.* 21, 4947-51, 2009.
- 26 21. Seow, Y., and Wood, M.J. Biological gene delivery vehicles: beyond viral vectors. *Mol. Ther.* 17,
- 27 767-77, 2009.
- 28 22. Gage, E., Hernandez, M.O., O'Hara, J.M., McCarthy, E.A., and Mantis, N.J. Role of the mannose
- 29 receptor (CD206) in innate immunity to ricin toxin. *Toxins* 3, 1131-45, 2011.
- 30 23. Wentworth, J.M., Naselli, G., Brown, W.A., Doyle, L., Phipson, B., Smyth, G.K., Wabitsch, M.,
- 31 O'Brien, P.E., and Harrison, L.C. Pro-inflammatory CD11c+CD206+ adipose tissue macrophages
- 32 are associated with insulin resistance in human obesity. *Diabetes* 59, 1648-56, 2010.
- 33 24. Wollenberg, A., Mommaas, M., Ooppel, T., Schottdorf, E.M., Gunther, S., and Moderer, M.
- 34 Expression and function of the mannose receptor CD206 on epidermal dendritic cells in
- 35 inflammatory skin diseases. *The Journal of Investigative Dermatology* 118, 327-34, 2002.
- 36 25. Canine, B.F., and Hatefi, A. Development of recombinant cationic polymers for gene therapy
- 37 research. *Adv Drug Deliv Rev* 62, 1524-9, 2010.
- 38 26. Eltoukhy, A.A., Siegwart, D.J., Alabi, C.A., Rajan, J.S., Langer, R., and Anderson, D.G. Effect of
- 39 molecular weight of amine end-modified poly(beta-amino ester)s on gene delivery efficiency and
- 40 toxicity. *Biomaterials* 33, 3594-603, 2012.
- 41 27. Bishop, C.J., Ketola, T.M., Tzeng, S.Y., Sunshine, J.C., Urtti, A., Lemmetyinen, H., Vuorimaa-
- 42 Laukkanen, E., Yliperttula, M., and Green, J.J. The effect and role of carbon atoms in poly(beta-
- 43 amino ester)s for DNA binding and gene delivery. *J. Am. Chem. Soc.* 135, 6951-7, 2013.
- 44 28. Jones, C.H., Chen, M., Ravikrishnan, A., Reddinger, R., Zhang, G., Hakansson, A.P., and Pfeifer,
- 45 B.A. Mannosylated poly(beta-amino esters) for targeted antigen presenting cell immune
- 46 modulation. *Biomaterials* 37, 333-44, 2015.
- 47 29. Doshi, N., and Mitragotri, S. Macrophages Recognize Size and Shape of Their Targets. *PLOS*
- 48 *One* 5, 2010.
- 49
- 50
- 51
- 52
- 53
- 54
- 55
- 56
- 57
- 58
- 59
- 60

Table of Contents Graphic

1  
2  
3  
4  
5  
6  
7  
8  
9  
10  
11  
12  
13  
14  
15  
16  
17  
18  
19  
20  
21  
22  
23  
24  
25  
26  
27  
28  
29  
30  
31  
32  
33  
34  
35  
36  
37  
38  
39  
40  
41  
42  
43  
44  
45  
46  
47  
48  
49  
50  
51  
52  
53  
54  
55  
56  
57  
58  
59  
60

